JOURNAL OF AIRCRAFT
Vol. 33, No. 2, March–April 1996

Vortex Wakes of Two Transports Measured in 80 by 120 Foot Wind Tunnel

V. J. Rossow,* R. K. Fong,† M. S. Wright,‡ and L. S. Bisbee§
NASA Ames Research Center, Moffett Field, California 94035-1000

Measurements are reported on the characteristics of the vortex wakes that trail from 0.03-scale models of a B-747 and a DC-10. Included are the downwash distributions obtained with a hot-film anemometer probe for the standard landing configurations, and the rolling moments induced on various following wings by the vortex wakes of several configurations of both wake-generating models. Both sets of data are presented for downstream distances of 81 and 162 ft, i.e., scale distances of 0.5 and 1.0 mile.

Nomenclature

AR = aspect ratio
b = wingspan, ft
c = wing chord, ft
C_L = lift coefficient, L/qS
C_l = rolling-moment coefficient, M/qSb
f = natural frequency, Hz
L = lift, lb
M = rolling moment, ft − lb
q = dynamic pressure, $\rho U_\infty^2/2$, lb/ft^2
r = radius, ft
S = wing planform area, ft^2
U_∞ = freestream velocity, ft/s
u, v, w = velocity components in x, y, and z directions, ft/s
x = distance in flight direction, ft
y = distance in spanwise direction, ft
z = distance in vertical direction, ft
α = angle of attack, deg
β = yaw angle, deg
Γ = bound circulation, ft^2/s
ρ = air density, slugs/ft^3

Subscripts

av = averaged over time at a given point
f = following model
g = wake-generating model
max = maximum on one side of centerline
mi = minimum at a given point
mx = maximum at a given point
p = pitch
r = roll

Introduction

THE objective of the NASA/Federal Aviation Administration (FAA) wake–vortex research program is to safely increase the rate at which aircraft can land and takeoff from a given runway. Such a program[1–5] was undertaken because the current capacity of airports is limited by the hazard posed by vortices that are shed by the wings of subsonic transport aircraft (Fig. 1), and not by some other aspect of traffic in the airport environment. Although the vortex wake of a lead aircraft induces lifting, yawing, and pitching motions on a following aircraft, the most hazardous feature of the wake occurs as an overpowering rolling moment near the center of a vortex.[2–8] For this reason, research into the characteristics of the vortex wakes produced by lift generation has concentrated on the structure of the wakes and, in particular, on the rolling moments that they induce on the following aircraft that encounter them.

Since flight tests are expensive to conduct and present experimental difficulties[7] when detailed measurements are desired on the characteristics of vortex wakes, a great deal of effort has gone into the use of ground-based facilities. Their use gained support when it was found that the results obtained in ground-based facilities agreed with the results from flight tests.[6,8] Work on the characteristics of the vortex wakes of subsonic transports began in the 40 by 80 ft Wind Tunnel[9–15] in the early 1970s. Recently,[16] the 80 by 120 ft Wind Tunnel was chosen as the facility for the investigation of wake vortices because it is now the largest NASA facility, and consequently, has the greatest downstream test distance (Table 1). The test section alone is long enough that wake measurements can be made at downstream distances that simulate scale distances up to 1 mile when models of 0.03 scale are used (Fig. 2). The first test in the 80 by 120 ft Wind Tunnel[16] showed that the measured results in the two large wind tunnels are in good agreement. On a continuing basis, the test data provide reliable data for the estimation of wake characteristics behind subsonic transports needed for airport capacity studies. In support of a basic research program on wake vortices, the test data were

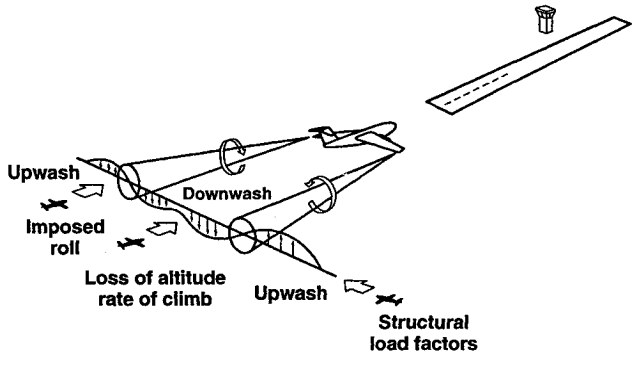

Fig. 1 Schematic of possible encounters with a lift-generated wake by a following aircraft.

Presented as Paper 95-1900 at the AIAA 13th Applied Aerodynamics Conference, San Diego, CA, June 19–22, 1995; received Aug. 15, 1995; revision received Nov. 6, 1995; accepted for publication Nov. 6, 1995.

*Senior Scientist, Low Speed Aerodynamics Branch, M/S N247-2. Associate Fellow AIAA.
†Aerospace Engineer, Wind Tunnel Operations Branch, M/S N221-5.
‡Instrumentation Engineer, Wind Tunnel Systems Branch, M/S N221-6.
§Design Engineer, M/S N226-3.

used to evaluate[17] a vortex–lattice method as a tool for estimating the lift and rolling-moment loads that are induced on following wings when the up- and downwash distributions are available. It was found that the method is quite accurate for following wings up to about one-fourth of the span of the wake-generating aircraft. At larger sizes of the following wing, the loads are overpredicted by increasing amounts because the vortex wake is distorted by the encountering wing.

As in the previous test in the 80 by 120 ft Wind Tunnel,[16] a 0.03-scale model of the Boeing 747 with a span of 70.5 in. is used as one of the wake-generating models. In the experiment being reported upon, a 0.03-scale model of the McDonnell Douglas DC-10 is also used. As noted in Table 2, the configurations tested include the conventional landing and several modifications of it to provide data for estimating the interaction of following aircraft with standard landing configurations, and to develop a database on how various wing-design parameters affect the wake–vortex structure and its decay with time or distance behind the wake-generating aircraft. To assess the characteristics of vortex wakes, following wings are tested or analyzed that range in size from 0.186 to 1.21 times the span of the wake-generating model (Table 3). Also, a two-component hot-film anemometer probe is used to determine the up- and downwash distributions in the wake at both the 81- and 162-ft downstream measuring stations.

Experimental Setup and Test Procedures

The present test setup is about the same as the one used in the previous 80 by 120 ft Wind Tunnel test,[16] and in the latter part of the 1970's test program[14,15] in the 40 by 80 ft Wind Tunnel at NASA Ames Research Center. One of the wake-generating models, B-747 or DC-10 (Table 2), is again mounted through a strain-gauge balance to a strut to measure the lift, drag, and pitching moment exerted on it by the freestream. Instead of locating the experiment on or near the centerline of the wind tunnel, as was done during the 40 by 80 ft Wind Tunnel tests, the models are now located off to the side of the 80 by 120 ft Wind Tunnel centerline (Fig. 2). The off-center mounting is used because the 80 by 120 ft Wind Tunnel merges with the circuit of the 40 by 80 ft Wind Tunnel along a diagonal junction. The constant area region is therefore longer on one side than on the other. Consequently, to maximize the downstream distance available for a test, the wake-generating models and following wings are mounted on that side of the test section (Fig. 2). The test-section length by itself is sufficiently long to allow separation distances between generator and follower up to about 200 ft. A 162 ft separation distance is achieved by locating the wake-generator in the forward part of the test section and the survey rig for the follower model at the end of the test section. As in the previous test in the 80 by 120 ft Wind Tunnel, an 81 ft separation distance is achieved by locating the generator model just off to the side of the turntable and not moving the following model and its traversing gear. In this way, the much larger and more cumbersome traverse mechanism that supports the following model need not move to change the separation distance.

An inverted mounting of the generator model is used to minimize interference of the strut wake with the vortex wake of the generator model (Fig. 3). The model wake then moves upward away from the strut wake, which tends to go straight downstream. The angle of attack of the wake-generating model

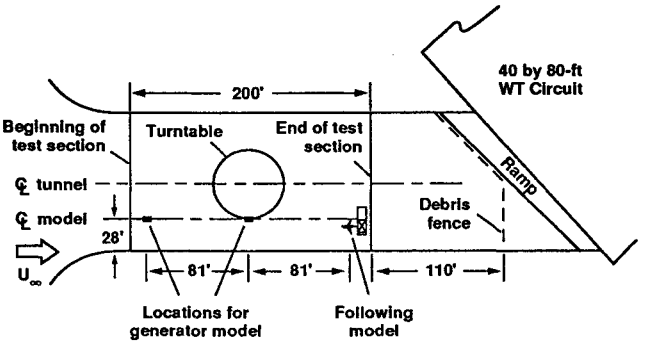

Fig. 2 Plan view of experiment in 80 by 120 ft Wind Tunnel.

Table 1 Wind-tunnel conditions

Freestream velocity, 131 ft/s
Dynamic pressure, 20 lb/ft^2
Distances to following models, 81 and 162 ft

Table 2 Data on wake-generating models

	B-747	DC-10
Scale of model	0.03	0.03
b_g	70.5 in.	59.5 in.
$\bar{c}_g$	10.1 in.	7.92 in.
Reynolds number ($\bar{c}_g$), Re_g	660,000	518,000
AR_g	6.96	7.5
S_g	4.94 ft^2	3.56 ft^2
Horizontal stabilizer angle	0 deg	0 deg
Landing gear and leading-edge slats extended		
Flaps in landing configuration inboard and outboard		

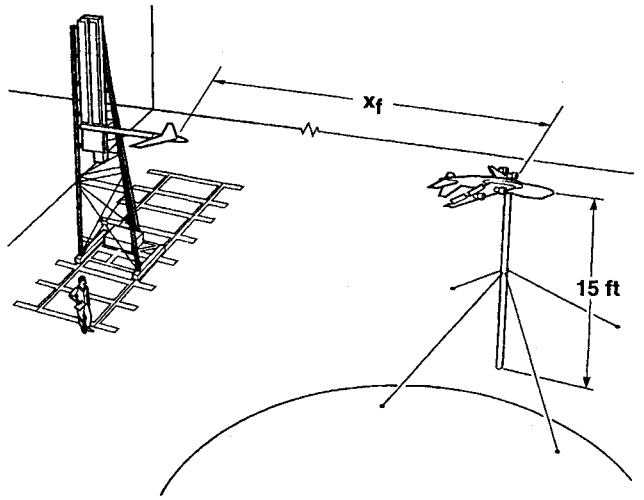

Fig. 3 Diagram of experiment in 80 by 120 ft Wind Tunnel.

Table 3 Data on following wings

No.	b_f, in.	c_{cL}, in.	c_{up}, in.	Λ_{LE}, deg	Λ_{TE}, deg	AR_f	S_f, ft^2	f_r, Hz	f_p, Hz
1	13.12	2.41	2.41	0	0	5.44	0.220	156	13.0
2	13.13	2.84	0.85	30	15	7.14	0.168	156	13.0
3	6.00	6.00	6.00	0	0	1.00	0.250	190	12.0
4	35.97	7.86	2.41	30	15	7.00	1.283	30.5	11.5
5	72.04	15.67	4.72	30	15	7.06	5.100	12.0	7.3

is set remotely through an actuator and indicator mechanism. The landing configurations of the wake-generating models (Fig. 4) include extended landing gear along with fully deployed leading-edge slats and trailing-edge flaps. Further details on the flaps and wing fins are presented in Refs. 13–16.

The models used as following wings are all made with a NACA 0012 airfoil section and have the planforms indicated in Table 3 and as shown in Fig. 5. The models are constructed of wood and aluminum, and then covered with fiberglass to ensure a smooth, durable finish along with structural rigidity and adequate frequency response. As a result, the natural frequencies in roll and pitch of the model–balance combinations are several times larger than the lift and rolling-moment frequencies encountered. The trailing model or wing is mounted on a sting (Fig. 3) that can be raised and lowered over a height range of about 8 ft. The vertical traverse mechanism is attached to a tower that can be translated laterally, or spanwise, across the airstream over a range of about 20 ft. The follower model is attached to its sting through a strain-gauge balance located inside the centerbody of the wing so that the wake-induced lift and rolling moment can be measured. The procedure used to take the data is the same as used in the previous test[16] in the 80 by 120 ft Wind Tunnel.

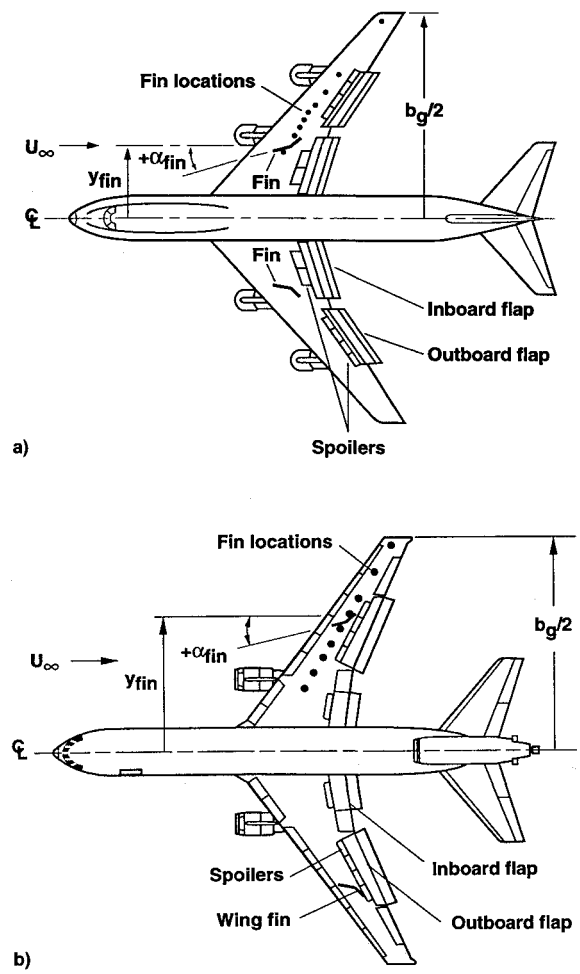

Fig. 4 Wake-generating models in plan view to illustrate flap arrangements and locations of wing fins: a) B-747 and b) DC-10.

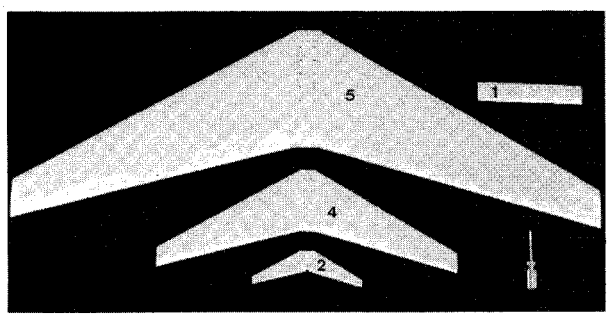

Fig. 5 Overhead photograph of following wings.

Results for Conventional Landing Configurations

The presentation of the results for the two wake-generating models is divided into two groups. The first group, which will be discussed in this section, includes the conventional landing configurations. The second group, which will be discussed in the next section, includes those configurations wherein modifications were applied to the wings of the wake-generating models in an effort to reduce the magnitude of the rotary velocities in the wake to alleviate the wake hazard for aircraft that might encounter them.

Up- and Downwash Distributions

The up- and downwash distributions are discussed first because their characteristics illustrate several features that affect the discussions of the rolling-moment measurements. Since the vertical velocity surveys require a large amount of time to acquire, they were restricted to only a few configurations that were chosen as being of most interest to the project. To facilitate making the best choice possible, the surveys were taken near the end of each test sequence so that the rolling-moment characteristics of the wakes shed by various configurations of the wake-generating models were available.

Consider first the distributions of flowfield angularity w/u behind the standard landing configurations of both wake-generating models at the two separation distances, $x_f = 81$ and 162 ft (Figs. 6a and 6b). In this article, only the lines connecting the measured data, and not the data points themselves, are presented to reduce the clutter on the graphs. Even though the data in Fig. 6 at $x_f = 162$ ft is not as smooth as the data at $x_f = 81$ ft, several observations can be made regarding changes in the vortex wakes with downstream distance. The increased noise in the velocity distributions at $x_f = 162$ ft is believed to

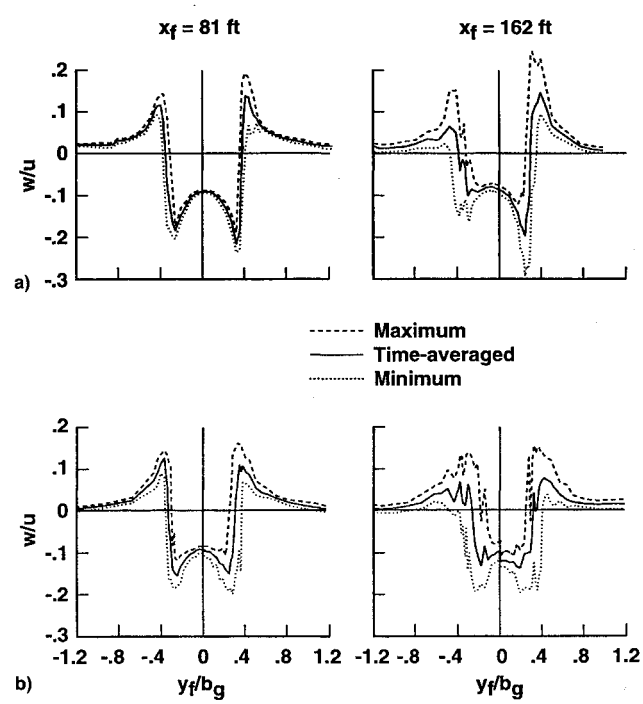

Fig. 6 Comparison of downwash distributions in wakes of transport models at two downstream distances: a) B-747; $\alpha_x = 4$ deg and b) DC-10; $\alpha_x = 8$ deg.

be caused by the larger meander distances, and therefore, the need for data sampling intervals longer than 1 min at $x_f = 162$ ft. As in the data presented previously,[16] the differences between the maximum and minimum data curves indicate not only the variations in the velocity at a given point in the flowfield, but also the lateral or spanwise displacement of the vortex center as it meanders about because of background turbulence in the airstream. Examination of the maximum and minimum curves in the vortex core region indicates that the vortex meanders about 4 in. (i.e., over about a 2 in. radius) at the 81-ft station, and about 8 in. (or over a 4 in. radius) at the 162-ft station. Such a variation is expected because the greater downstream distance allows twice as much time for the turbulent eddies to convect and distort the vortices from their time-averaged locations. Since the analog data coming from the hot-film anemometer are filtered at 0.1 Hz, vortex excursions with a higher frequency do not appreciably influence the recorded data. At 0.1 Hz, the wavelength of an eddy in the airstream is about 13 ft (i.e., between 2–3 span lengths).

After the data were plotted, it was quite surprising to find that some of the swirl velocities in the vortices were noticeably higher at $x_f = 162$ ft than at $x_f = 81$ ft (Figs. 6a and 6b). These downwash profiles indicate vortex intensification rather than decay. In contradiction, the measured rolling moments to be presented in figures to follow were always less at the $x_f = 162$-ft station than at the $x_f = 81$-ft station, which is an indication of some vortex decay. Therefore, the two sets of data appear to be inconsistent, because rolling moments calculated by use of the measured velocity distributions would be significantly larger than the measured ones, at either the $x_f = 162$-ft station or the $x_f = 81$-ft station. A variety of explanations for this inconsistency in the measured data were explored. The one that seemed to best represent the observed characteristics of the data appears to be related to the way in which the hot-film anemomenter data were taken, and to possible vortex stretching by the turbulence eddies in the freestream flowfield. The time-averaged data presented in Fig. 6 represent the measurements taken during a 1-min interval at a given point, while the vortex center moves about randomly. In the data-taking process, the 1-min interval is divided into 0.1-s intervals to yield 600 data samples. The maximum and minimum data points are obtained as the two extremities of the 600 samples taken during the 1-min interval. If the wind-tunnel airstream had no turbulence, the time-averaged, maximum, and minimum data would all be the same. But since the wind-tunnel airstream does contain turbulence, the vortex moves about (meanders), and is stretched and compressed to change the magnitude of the swirl velocities in the vortex, thereby leading to the three curves in each part of Fig. 6.

To understand the effect of the meander and of the stretching processes, consider the hypothetical case where the vortex meanders, but does not stretch or compress to change its intensity. If such a situation existed, the peak magnitudes of the maximum (and the minimum) curve would be the same over a lateral distance equal to the meander distance. The magnitudes, of course, would be a combination of the maximum swirl velocity of the vortex and the induced velocity of the other vortex in the pair. This points out the fact that the maximum and minimum curves represent the envelope of velocity profiles for all possible meander locations of the vortex and not the instantaneous downwash profile. As the meander distance increases, the flat top and bottom of the two extremity curves also increases. If the total area under the velocity curves is used to compute rolling moment, a sizeable error will occur. Therefore, when the maximum and minimum curves are combined for a single downwash velocity distribution, the lateral offsets because of meander are removed.

Now consider the second hypothetical case wherein the vortex is stretched, but its center is not displaced from the measuring point during the measuring interval. Such a situation arises whenever eddies in the airstream combine to bend and stretch the vortex locally, but do not move the vortex center from its time-averaged location. Both extremities of the velocity curves are then increased because vortex stretching reduces the core radius while retaining the angular momentum of the flowfield. The imposed rolling moment is not changed appreciably, if at all, even though the maximum swirl velocity has been increased because the intensification occurs within the core at a small radius so that the following wing does not experience much increase in torque. (Large amounts of vortex curvature and stretching can change the vortex structure substantially, but amounts that large are not expected for ordinary wind-tunnel turbulence, at the distances used in the present test.) Since the maximum and minimum curves in Fig. 6 are made up of the envelopes of the extremities of the data taken at each survey point, they would include all of the enhanced velocity variations caused by vortex stretching. The complexity of the interaction of the vortices with the airstream turbulence makes it difficult to estimate the amount of vortex enhancement, but it seems that the process could account for the larger velocities at the $x_f = 162$-ft station. That is, it is conjectured that both meander and vortex stretching occur to form an envelope of the maximum and minimum velocity curves. As the amplitude of vortex meander increases, the amplitude of the velocity extremes also increases. Further evidence of vortex stretching was believed to occur in the data when values of rolling moment were found at the periphery of the meander region rather than at the time-averaged location of the vortex center. On-line observation of the data indicated that the analog signals were much more erratic at the $x_f = 162$-ft station than at the $x_f = 81$-ft station, just as illustrated in Fig. 6. It is believed that a series of experiments designed to explore the foregoing conjectures will clarify the various characteristics in the data associated with vortex meander and stretching, and will resolve the inconsistencies in the data. It should be remembered that, as aggravating as vortex meander is in the wind tunnel when valid measurements are desired, the same or similar phenomenon is also present in the atmosphere. An improved understanding of how turbulence affects the intensity and decay of vortices is therefore needed to predict their behavior in the airport environment.

Effect of Yaw of the Wake-Generating Model

The first sequence of runs carried out during the recent wind-tunnel entry examined the effects of yaw on the relative strengths of the port and starboard sides of the wake. The sequence of runs was carried out only with the B-747 wake-generating model at 4-deg angle of attack and with following wing no. 1. The purpose of the experiment was to determine how much, if any, the vortex wake of the aircraft model was changed because of yaw. Such a question was raised by previous tests, which noted a significant difference in the port and starboard magnitudes of the rolling moment imposed on following models, even though the model was aligned with the wind-tunnel centerline to within about ± 0.1 deg. To be sure that the asymmetry in the wake was not caused by small errors in yaw placement of the wake-generating model, tests were carried out at yaw angles of $\beta = -2$, 0, and $+2$ deg. A 2-deg increment was chosen because it far exceeds the accuracy with which the yaw angle of the model can be placed during the setup of the experiment. The results presented in Fig. 7 show that small angles of yaw do not account for the asymmetries in the structure of the lift-generated vortices. It is concluded therefore that structural differences in the two sides of the model cause the vortex wakes to differ by as much as they do on the port and starboard sides. Since the data in Fig. 7 indicate a small change in rolling moment with yaw, the remainder of the tests were conducted with the model aligned with the centerline of the wind tunnel to within an estimated accuracy of about ± 0.1 deg.

Effect of Angle of Attack of the Wake-Generating Model

In the past, only a few run sequences were carried out wherein the angle of attack α_g was varied. As indicated in Figs.

8a and 8b, and as expected, the magnitude of the rolling moments induced on following wing no. 1 by the wake increase as the lift increases. The results for both the B-747 and the DC-10 at x_f = 81 and 162 ft are offset indicating that some wake decay probably occurred. The larger differences at the lower angles of attack are believed to be caused by the turbulence introduced into the wake by the slats and flaps that operate there at significantly off-design conditions. Past experience has shown that the introduction of turbulence into the wake causes the measured rolling moments to decrease significantly. Unfortunately, a limit appears to exist beyond which further introduction of turbulence does not reduce the wake hazard, but does significantly affect the performance of the generator aircraft.[12] At the upper end of the angle-of-attack range, the rolling moments are about the same at the two

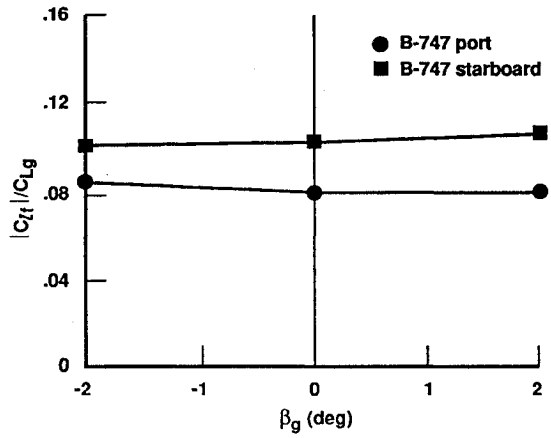

Fig. 7 Effect of yaw angle on measured rolling moment in wake of B-747; α_g = 4 deg, C_{L_g} = 1.2; following model no. 1; x_f = 81 ft.

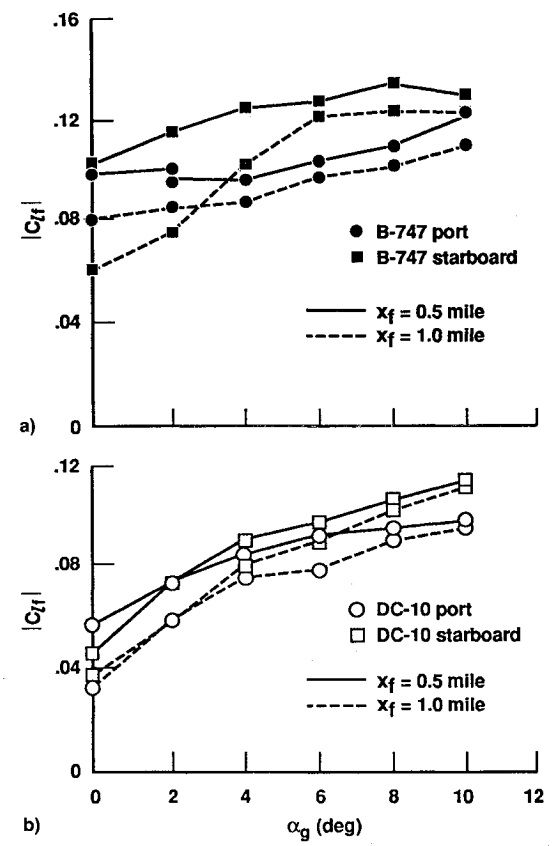

Fig. 8 Maximum rolling moment $|C_{lf}|$ induced on following wing no. 1 by wakes of the standard landing configurations as a function of angle of attack: a) B-747 and b) DC-10.

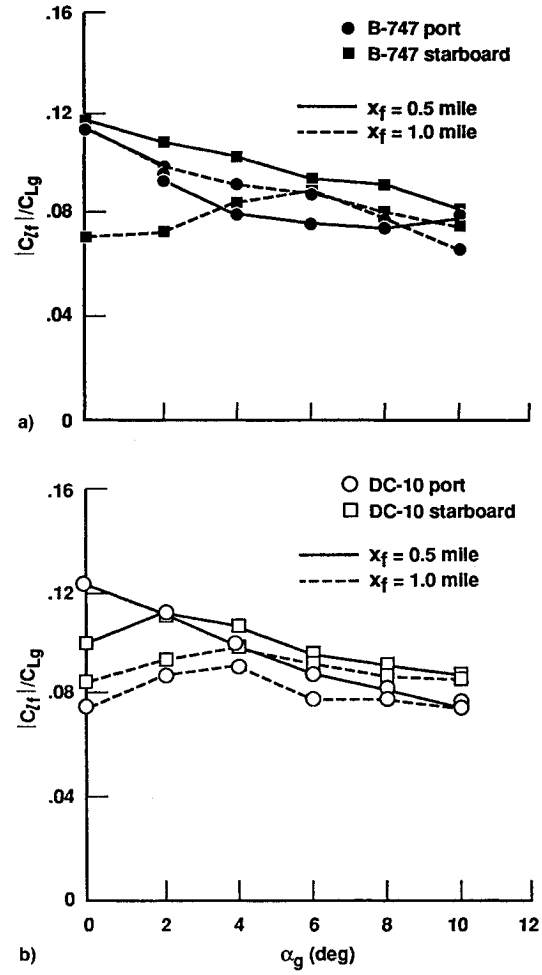

Fig. 9 Reduced maximum rolling moment $|C_{lf}|/C_{L_g}$ induced on following wing no. 1 by wakes of the standard landing configurations as a function of angle of attack: a) B-747 and b) DC-10.

downstream stations, indicating that wake decay is small when the wake-generating wing is operating at near-design conditions.

A characteristic not observed in previous tests is a small amount of hysteresis that occurs in the lift on the generator model as the angle of attack is approached from above rather than from below. Once this characteristic was identified, the angle of attack on the generator model was set by approaching the desired angle from above. In this way, the lift at a given angle of attack was the greatest obtained at a given angle of attack. The angle of attack is determined by an indicator fastened to the inside of the wake-generating model to eliminate uncertainty in the angle of attack because of freedom of movement in the drive linkage.

If only the intensity of (and not the distribution within) the vortex changes with angle of attack, the maximum rolling moment induced on a following wing would be proportional to the lift on the wake-generating wing. To test this possibility, the ratio of rolling moment to lift $|C_{lf}|/C_{L_g}$ is plotted as a function of the angle of attack (Fig. 9). In both cases, a linear relationship appears not to exist. Some of the reasons for the nonlinearity may be caused by flow separation on the wake-generating wings at low angles of attack. It is believed, however, that the primary cause is attributable to the changes in span loading as the angle of attack changes. The span loading changes with angle of attack because the inboard parts of wings have large flap deflections and the outboard parts do not.

A direct comparison of the wake-induced rolling moments of the two wake-generating models suggests that, at a given

angle of attack, the larger B-747 has a somewhat more intense wake than the DC-10 (Fig. 10a). The more appropriate way in which to compare the results, which removes the sensitivity to C_{Lg}, is to plot the ratio $|C_{lf}|/C_{Lg}$ as a function of the angle of attack (Fig. 10b). The rolling-moment intensity of the two wakes then appears to be comparable. The descent distances of the vortices below the generating wing at the 162-ft station were approximately twice the amounts measured for the 81-ft station (see also, Table 4 of Ref. 16 for data at α_g = 4 deg), becoming about $1.1b_g$ at α_g = 10 deg for both the DC-10 and the B-747. Since the DC-10 produces less lift at the smaller angles of attack, its vortices only descended about $0.3b_g$ at α_g = 0 deg, whereas the vortices of the B-747 descended about $0.7b_g$ at the 162-ft station.

The effect of the size of the following wing on its susceptibility to a vortex wake is illustrated by plotting the wake-induced rolling moments as a function of the span ratio b_f/b_g (Fig. 11a). The ratio of rolling moment to the lift tends to deemphasize the effect of lift coefficient on the results, and the use of span ratio on the abscissa tends to account for the difference in relative size of the two aircraft models.[19] Also included in Fig. 11 are two dashed curves that were obtained by use of the up- and downwash curves in Fig. 6b at the 81-ft station for the DC-10 wake-generating model as input for a vortex–lattice code.[17] As pointed out in Ref. 17, the method overpredicts the maximum rolling moments by about 10–15% when the following wing is about one-half the size of the generating wing, and about 30% when the two wings are about equal. Therefore, the fact that the computed values are above

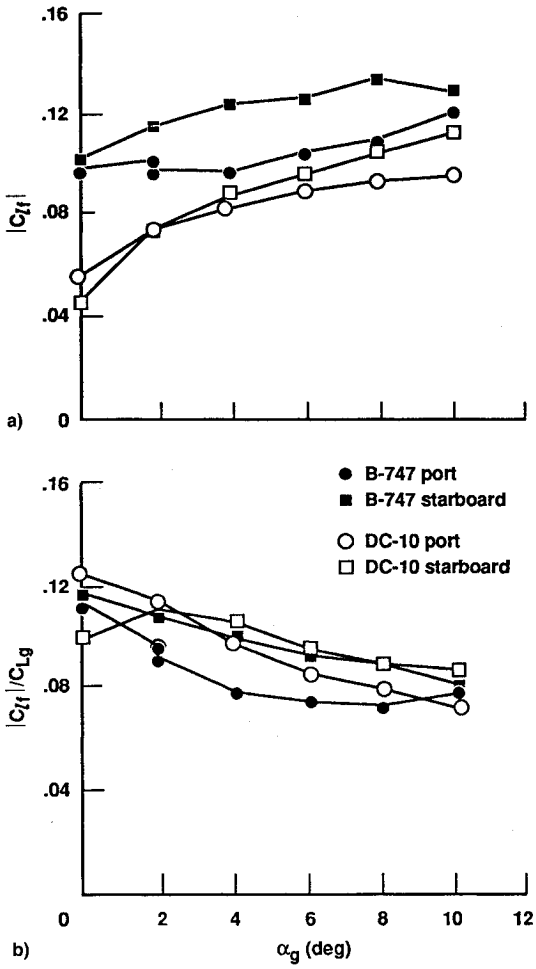

Fig. 10 Comparison of maximum rolling moments induced on following wing no. 1 by wakes of the two wake-generating models in their standard landing configuration; x_f = 81 ft: a) $|C_{lf}|$ and b) $|C_{lf}|/C_{Lg}$.

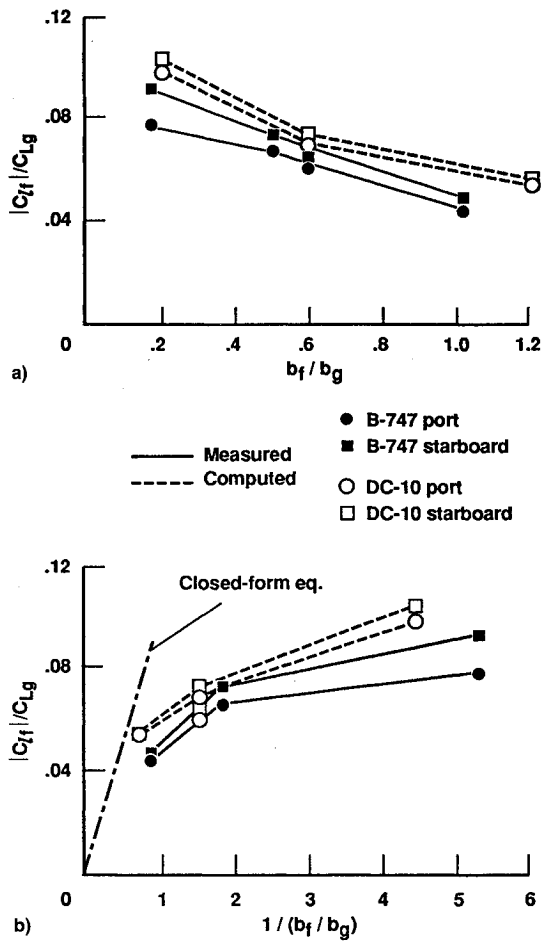

Fig. 11 Comparison of wake-induced rolling moments on swept following wing nos. 2, 4, and 5 as a function of span ratio and inverse span ratio; x_f = 81 ft: a) b_f/b_g and b) b_g/b_f.

the measured ones is attributable at least partly to the computational method. As mentioned previously, the predicted rolling moments may also be too large because the downwash profiles may include effects of vortex stretching that cause the velocities to be larger than should be associated with a stationary vortex.

The use of the inverse span ratio b_g/b_f is useful for comparison because an estimate for the lift and rolling moment induced by a line vortex (i.e., all circulation concentrated at the center) has been derived in closed form.[19] The expressions for the maximum values are given by

$$C_{Lf\,\max} = \mathrm{AR}_f(\Gamma_v/b_g U_\infty)(b_g/b_f) \quad (1)$$

$$C_{lf\,\max} = (\mathrm{AR}_f/8)(\Gamma_v/b_g U_\infty)(b_g/b_f) \quad (2)$$

Since Eq. (2) is a linear function of b_g/b_f, an estimate for the maximum rolling moment induced on a wing by a line vortex is a straight line through the origin in Fig. 11b. The deviation of the curve through the present data from the straight line indicates the decrease in rolling moment brought about by a span loading that is not rectangular; i.e., a vortex with its circulation distributed around, rather than concentrated at, the center. Extrapolation of the experimental data to b_g/b_f = 0 indicates that the closed-form expression, Eq. (2), has the correct form.

Results for Alleviated Landing Configurations

Another way in which to compare the wakes of aircraft is to explore how sensitive or susceptible their lift-generated wakes are to changes in the planform of, or to devices attached

to, their wings. The objective here is to determine whether changes in the B-747 that were found to be successful in previous tests[13,16,20] would also be more or less successful in reducing the intensity of the rotary velocities in the wake of the DC-10 model. The use of such devices is only of interest when the aircraft is in its landing or takeoff configuration, because reduction of the wake hazard is only needed in the vicinity of airports while aircraft are landing or departing, which is when they are constrained to the same flight corridor. Various devices have been studied rather extensively with a model of the B-747 (Refs. 13–16), but the recent test in the 80 by 120 ft Wind Tunnel appears to be the only exploration with wing fins and with various arrangements of trailing-edge flaps on a DC-10 model.

Effect of Span of Trailing-Edge Flaps

Early in the wake–vortex research program of the 1970s, it was discovered that the wake intensity of the B-747 could be substantially reduced by changing the standard landing configuration to the so-called (30- and 0-deg) flap configuration.[3–8,13] The configuration is achieved by placing the inboard flaps in their standard landing configuration and the outboard flaps in their stowed position. In the recent test, configurations were tested on both the B-747 and the DC-10 models wherein the spanwise extent of the outboard flap is varied. In this way, the configurations tested include, at one limit, the outboard flap as fully stowed, and at the other limit fully deployed. The intermediate spanwise flap sizes that were tested include lengths of the deployed flap of 25, 50, and 75% of the standard length (Fig. 4). Once again, to reduce the influence of the magnitude of the lift on the rolling-moment data, the data are presented as $|C_{lf}|/C_{L_g}$ in Fig. 12. The measured data show that the maximum value of the induced rolling moment is a minimum when the outboard flap is completely stowed [e.g., the (30- and 0-deg) flap configuration of the B-747]. The higher value of rolling moment on the port side is consistently observed with this model, and is believed to be caused by the fact that the alleviation mechanism did not go to completion within the 81 ft distance from the generator to the following model. The maximum rolling moments are noted to be largest when both flaps are fully deployed. The test results also indicate that intermediate flap sizes are not preferred. It was not possible to determine whether the vortex-linking mechanism attributed to the alleviation on the B-747 (Ref. 20) also applies to the DC-10.

Effect of Wing Fins

The mechanism by which lift-generated wakes are alleviated when vertical surfaces (wing fins) are placed on the upper surface of wings is not clearly defined. It is, however, the one wake-alleviation scheme that has indicated substantial reductions in the wake-induced rolling moments for the B-747 model when it was tested over a range of wing-fin configurations[14–16]; see the curve in Fig. 13 that represents previous data. Since a formulation for the mechanism has not been found, extension of the wing–fin scheme to the wake-generating wing in a way that makes the penalties in performance negligible has not been found. (Typical lift and drag penalties associated with wing fins are illustrated in Fig. 4 of Ref. 16.) It is still of interest to apply the wing–fin concept to the DC-10 to determine its characteristics and potential level of effectiveness.

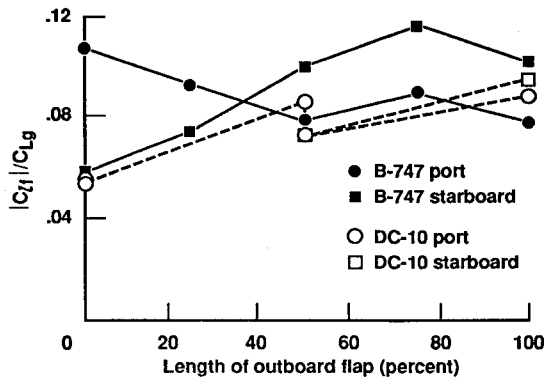

Fig. 12 Variation of wake-induced rolling moment with spanwise size of outboard trailing-edge flaps; following model no. 1, x_f = 81 ft; B-747, α_g = 4 deg; DC-10, α_g = 6 and 8 deg.

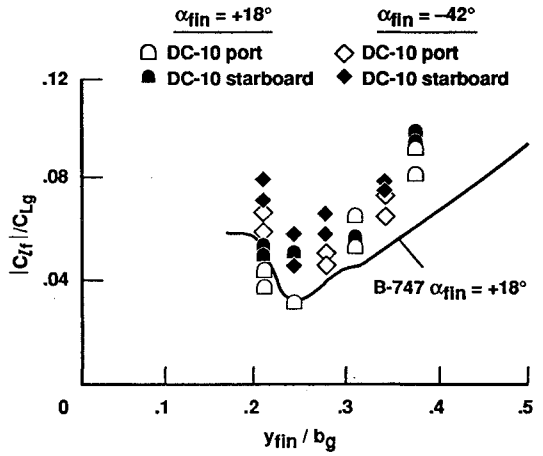

Fig. 13 Variation of wake-induced rolling moment with spanwise location of fins mounted on upper surface of wings; following model no. 1, x_f = 81 ft.

The curve in Fig. 13 for the rolling moment as a function of spanwise location of a fin on the B-747 wing indicates that the optimum location for a fin is near the halfway point between the wingtip and centerline.[14–16] A similar result is also found for the DC-10 model (Fig. 13), whether the fin is at a positive or negative angle of attack. A difference occurs in the preferred magnitude of the angle of attack of the fin because, as a result of wing sweep, the flow direction over the upper surface of the wing where the fin is located has a strong inboard component. The optimum spanwise location is about the same on both aircraft models, but the magnitudes differ. The differences may be because of the nature of the two wings, but it is believed to be more likely from a difference in the relative sizes of the two sets of fins used in the experiment. That is, when the B-747 model was tested, the fin size was 0.0567 by $0.0851b_g$. When the DC-10 model was tested, the fin size was 0.0336 by $0.0672b_g$. The smaller relative fin size was used on the DC-10 because larger sizes degraded the performance a disproportionate amount. It is concluded that the mechanism of wake alleviation by wing fins is probably the same on the two wake-generating models, and that the magnitudes can be made comparable by changes in the fin design. The approximately equal effectiveness of the fins on the two models is not surprising. Although the two wing planforms appear to differ somewhat, both were no doubt designed for minimum weight at a given lift to yield quite similar span-load distributions. If such is the case, the span loadings and the vortex wakes shed by the two models are similar enough that they are about equally susceptible to the influence of wing fins.

Concluding Remarks

The data presented on the two wake-generating models indicates that their vortex wakes are comparable when the size of the aircraft and the lift on the wings are taken into consideration. It is also found that the vortex wakes of both models are susceptible to alleviation in about the same way and to about the same degree when the trailing-edge flaps or wing fins are employed for optimum effectiveness.

The rolling-moment data taken at the two downstream distances (which correspond to $\frac{1}{2}$- and 1-mile distances at full

scale), indicate that some decay in the intensity of the vortices does occur at the time-averaged locations of the vortices. Inconsistent with this result are the large values obtained for the measured downwash velocity distribution at x_f/b_g = 162-ft station. It is believed that the higher velocities are brought about by vortex stretching that occurs as the vortex becomes more sinuous at the larger downstream distance, and by the way that the data were taken.

References

[1]Hallock, J. N., "Aircraft Wake Vortices: An Annotated Bibliography (1923–1990)," U.S. Dept. of Transportation, John A. Volpe National Transportation Systems Center, Rept. DOT-FAA-RD-90-30, DOT-VNTSC-FAA-90-7, Cambridge, MA, Jan. 1991.

[2]Olsen, J. H., Goldburg, A., and Rogers, M. (eds.), *Aircraft Wake Turbulence and Its Detection*, Plenum, New York, 1971.

[3]"NASA Symposium on Wake Vortex Minimization," NASA SP-409, 1976.

[4]Hallock, J. N. (ed.), *Proceedings of the Aircraft Wake Vortices Conference*, U.S. Dept. of Transportation, FAA-RD-77-68, 1977, pp. 6–31.

[5]Wood, W. D. (ed.), *FAA/NASA Proceedings Workshop on Wake Vortex Alleviation and Avoidance*, U.S. Dept. of Transportation, FAA-RD-79-105, 1978, pp. 1-1–1-42.

[6]Smith, H. J., "A Flight Test Investigation of the Rolling Moments Induced on a T-37B Airplane in the Wake of a B-747 Airplane," NASA TM-56031, April 1975.

[7]Jacobsen, R. A., and Short, B. J., "A Flight Investigation of the Wake Turbulence Alleviation Resulting from a Flap Configuration Change on a B-747 Aircraft," NASA TM-73,263, July 1977.

[8]Barber, M. R., and Tymczyszyn, J. J., "Wake Vortex Attenuation Flight Tests: A Status Report," *1980 Aircraft Safety and Operating Problems Conference*, Pt. 2, NASA Langley Research Center, March 1981, pp. 387–408.

[9]Corsiglia, V. R., Schwind, R. G., and Chigier, N. A., "Rapid Scanning, Three-Dimensional Hot-Wire Anemometer Surveys of Wing Tip Vortices," *Journal of Aircraft*, Vol. 10, No. 12, 1973, pp. 752–757.

[10]Rossow, V. J., Corsiglia, V. R., and Philippe, J. J., "Measurements of the Vortex Wakes of a Subsonic- and a Supersonic-Transport Model in the 40- by 80-Foot Wind Tunnel," NASA TM X-62,391, Sept. 1974.

[11]Rossow, V. J., Corsiglia, V. R., Schwind, R. G., Frick, J. K. D., and Lemmer, O. J., "Velocity and Rolling-Moment Measurements in the Wake of a Swept-Wing Model in the 40- by 80-Foot Wind Tunnel," NASA TM X-62,414, April 1975.

[12]Corsiglia, V. R., and Rossow, V. J., "Wind-Tunnel Investigation of the Effect of Porous Spoilers on the Wake of a Subsonic Transport Model," NASA TM X-73,091, Jan. 1976.

[13]Corsiglia, V. R., Rossow, V. J., and Ciffone, D. L., "Experimental Study of the Effect of Span Loading on Aircraft Wakes," *Journal of Aircraft*, Vol. 13, No. 12, 1976, pp. 968–973.

[14]Rossow, V. J., "Effect of Wing Fins on Lift-Generated Wakes," *Journal of Aircraft*, Vol. 15, No. 3, 1978, pp. 160–167.

[15]Rossow, V. J., "Experimental Investigation of Wing Fin Configurations for Alleviation of Vortex Wakes of Aircraft," NASA TM 78520, Nov. 1978.

[16]Rossow, V. J., Sacco, J. N., Askins, P. A., Bisbee, L. S., and Smith, S. M., "Wind-Tunnel Measurements of Hazard Posed by Lift-Generated Wakes," *Journal of Aircraft*, Vol. 32, No. 2, 1995, pp. 278–284.

[17]Rossow, V. J., "Validation of Vortex-Lattice Method for Loads on Wings in Lift-Generated Wakes," *Journal of Aircraft*, Vol. 32, No. 6, 1995, pp. 1254–1262.

[18]Zeman, O., "Persistence of Trailing Vortices: A Modeling Study," *Physics of Fluids*, Vol. 7, No. 1, 1995, pp. 135–143.

[19]Rossow, V. J., "Estimate of Loads During Wing-Vortex Interactions by Munk's Transverse-Flow Method," *Journal of Aircraft*, Vol. 27, No. 1, 1990, pp. 66–74.

[20]Rossow, V. J., "Prospects for Alleviation of Hazard Posed by Lift-Generated Wakes," *Proceedings of the Aircraft Wake Vortices Conference*, edited by J. N. Hallock, Vol. 1, U.S. Dept. of Transportation, Federal Aviation Administration, DOT/FAA/SD-92/1.1, DOT-VNTSC-FAA-92-7.1, Washington, DC, 1991, pp. 1–40 (Paper 22).